

LETTER • OPEN ACCESS

## Ocean acidification in emission-driven temperature stabilization scenarios: the role of TCRE and non-CO<sub>2</sub> greenhouse gases

To cite this article: Jens Terhaar *et al* 2023 *Environ. Res. Lett.* **18** 024033

View the [article online](#) for updates and enhancements.

You may also like

- [A framework to understand the transient climate response to emissions](#)  
Richard G Williams, Philip Goodwin, Vassil M Roussenov *et al.*
- [Uncertainty in carbon budget estimates due to internal climate variability](#)  
Katarzyna B Tokarska, Vivek K Arora, Nathan P Gillett *et al.*
- [Much of zero emissions commitment occurs before reaching net zero emissions](#)  
Charles D Koven, Benjamin M Sanderson and Abigail L S Swann

ENVIRONMENTAL RESEARCH  
LETTERS

## LETTER

Ocean acidification in emission-driven temperature stabilization scenarios: the role of TCRE and non-CO<sub>2</sub> greenhouse gases

## OPEN ACCESS

## RECEIVED

28 October 2022

## REVISED

20 December 2022

## ACCEPTED FOR PUBLICATION

3 January 2023

## PUBLISHED

2 February 2023

Original content from this work may be used under the terms of the [Creative Commons Attribution 4.0 licence](#).

Any further distribution of this work must maintain attribution to the author(s) and the title of the work, journal citation and DOI.

Jens Terhaar<sup>1,2,3,\*</sup> , Thomas L Frölicher<sup>1,2</sup>  and Fortunat Joos<sup>1,2</sup> <sup>1</sup> Climate and Environmental Physics, Physics Institute, University of Bern, Bern, Switzerland<sup>2</sup> Oeschger Centre for Climate Change Research, University of Bern, Bern, Switzerland<sup>3</sup> Department of Marine Chemistry and Geochemistry, Woods Hole Oceanographic Institution, Woods Hole, MA 02543, United States of America

\* Author to whom any correspondence should be addressed.

E-mail: [jens.terhaar@unibe.ch](mailto:jens.terhaar@unibe.ch)**Keywords:** ocean acidification, Paris Agreement, uncertaintiesSupplementary material for this article is available [online](#)**Abstract**

Future ocean acidification mainly depends on the continuous ocean uptake of CO<sub>2</sub> from the atmosphere. The trajectory of future atmospheric CO<sub>2</sub> is prescribed in traditional climate projections with Earth system models, leading to a small model spread and apparently low uncertainties for projected acidification, but a large spread in global warming. However, climate policies such as the Paris Agreement define climate targets in terms of global warming levels and as traditional simulations do not converge to a given warming level, they cannot be used to assess uncertainties in projected acidification. Here, we perform climate simulations that converge to given temperature levels using the Adaptive Emission Reduction Algorithm (AERA) with the Earth system model Bern3D-LPX at different setups with different Transient Climate Response to cumulative carbon Emissions (TCRE) and choices between reductions in CO<sub>2</sub> and non-CO<sub>2</sub> forcing agents. With these simulations, we demonstrate that uncertainties in surface ocean acidification are an order of magnitude larger than the usually reported inter-model uncertainties from simulations with prescribed atmospheric CO<sub>2</sub>. Uncertainties in acidification at a given stabilized temperature are dominated by TCRE and the choice of emission reductions of non-CO<sub>2</sub> greenhouse gases (GHGs). High TCRE and relatively low reductions of non-CO<sub>2</sub> GHGs, for example, necessitate relatively strong reductions in CO<sub>2</sub> emissions and lead to relatively little ocean acidification at a given temperature level. The results suggest that choices between reducing emissions of CO<sub>2</sub> versus non-CO<sub>2</sub> agents should consider the economic costs and ecosystem damage of ocean acidification.

**1. Introduction**

The Paris Agreement aims at limiting global warming well below 2 °C and at pursuing efforts to reduce warming to 1.5 °C to significantly reduce the risks and impacts of climate change [1]. To stabilize temperatures, the sum of CO<sub>2</sub> forcing equivalent (CO<sub>2</sub>-fe) emissions [2, 3] from all greenhouse gases (GHGs) together must be close to net-zero [4–7]. The remaining allowable emissions of CO<sub>2</sub> and non-CO<sub>2</sub> forcing agents that can be emitted before net-zero must be reached depends among others on the Transient Climate Response to Cumulative Emissions (TCRE), i.e. the amount of warming per amount of cumulative

emissions. TCRE depends on the transient climate response (or Equilibrium Climate Sensitivity (ECS)) and the strength of the ocean and land carbon sinks [2, 5, 8–16]. These allowable emissions can be distributed over all GHGs in many combinations. If relatively strong reductions in non-CO<sub>2</sub> GHG emissions would be implemented, for example, the remaining allowable CO<sub>2</sub> emissions will be relatively higher.

Globally averaged atmospheric surface warming is the main and often only measure of success or failure of the Paris Agreement, although climate impacts and stressors of ecosystems do not only or sometimes not at all depend on the level of global warming [17–19]. One example of such a potential ecosystem

stressor is ocean acidification, a process that describes the gradual decrease in ocean pH, carbonate ions, and calcium carbonate mineral saturation states ( $\Omega$ ) in the ocean, which affects a variety of individual calcifying marine organisms and has the potential to disrupt entire ecosystems [20–30].

Future ocean acidification depends mainly on CO<sub>2</sub> emissions and the perturbation in atmospheric and oceanic carbon cycle and is only marginally affected by the degree of warming [31], except in the Arctic Ocean [31, 32]. In surface waters, equilibrating rapidly with the atmosphere, acidification is primarily driven by atmospheric CO<sub>2</sub> [23, 24, 33], with a regional role for alkalinity changes, e.g. in estuaries and the Arctic Ocean [34–38]. Acidification at depth depends mainly on how much of the anthropogenic carbon perturbation at the surface is transported to the deeper ocean [39–43].

As trajectories of future atmospheric CO<sub>2</sub> are prescribed in the simulations from the Coupled Model Intercomparison Project (CMIP) by the socioeconomic pathways [44, 45] that are used by the regular IPCC reports [46, 47], projections of ocean acidification have usually very low to non-existent model uncertainties at the ocean surface [18, 19, 33, 37, 48]. Therefore, these simulations cannot directly be used to inform policy makers about the uncertainties in ocean acidification and might, in the worst case, lead to overly confident projections on ocean acidification used for impact assessments. Only few studies assess uncertainties in projected ocean acidification comprehensively with prescribed carbon emissions by using perturbed parameter ensembles in simulations or by quantifying uncertainties as a function of cumulative carbon emissions [17, 49, 50]. These studies quantify uncertainties related to the land and ocean carbon sink but neither quantify uncertainties from the choice of GHG reductions (CO<sub>2</sub> vs non-CO<sub>2</sub>) nor from the transient climate response to emissions. Such studies that quantify global ocean acidification and related uncertainties at a given level of global warming for different choices of GHG emission reductions remain missing.

The magnitude of ocean acidification and the associated uncertainty at a given stabilized temperature level can, however, be determined by simulations that adapt GHG emissions successively to converge to the same stabilized warming level. Such simulations prescribe the future warming level and not the atmospheric CO<sub>2</sub> trajectories and hence do not quantify the uncertainty of warming per increase of atmospheric CO<sub>2</sub> but the uncertainty of increases of atmospheric CO<sub>2</sub> per warming. Approaches like the adjusting mitigation pathway (AMP) approach [51, 52] or the recently developed Adaptive Emission Reduction Approach (AERA) [53] allow to make such simulations with Earth system models by developing dynamically emission curves, which stabilize the simulated warming at any chosen temperature target.

Here, we use the AERA, which accounts for all radiative agents and not only for CO<sub>2</sub> as the AMP, in combination with a reduced-form atmospheric chemistry model and the Earth system model of Intermediate Complexity Bern3D-LPX with varying climate sensitivities and ocean mixing rates [54, 55] to quantify ocean acidification when warming stabilized at 1.5 °C, 2.0 °C, 2.5 °C, and 3.0 °C above preindustrial temperature and the uncertainty due to varying TCREs, and the choice of reductions in CO<sub>2</sub> and non-CO<sub>2</sub> GHG emission. We use different configurations of Bern3D-LPX as a surrogate for a typical CMIP ensemble of Earth System Models (ESMs). The wide range of simulations with the AERA demonstrates that the main uncertainty of ocean acidification projection for a given warming stems mainly from the uncertainty in the knowledge of TCRE and the choice in the reductions in non-CO<sub>2</sub> emissions. Moreover, the AERA simulations with Bern3D-LPX underline the importance of emission-driven temperature stabilization simulations in the CMIP framework for projections and uncertainty assessments of the Earth system, its carbon cycle [56], extreme events [43, 57], and ecosystem stressors [19] in a stabilized climate.

## 2. Methods

### 2.1. Adaptive emission reduction approach (AERA)

The AERA estimates a future trajectory of CO<sub>2</sub>-fe emissions [2, 3, 10] that allows to stabilize the global atmospheric surface warming at a prescribed temperature level in three steps solely based on past annually averaged trajectories of (a) CO<sub>2</sub> emissions, (b) atmospheric CO<sub>2</sub>, (c) the radiative forcing of all non-CO<sub>2</sub> forcing agents, and (d) global mean surface temperatures [53].

First, the AERA estimates the anthropogenic warming from the time series of radiative forcing and temperatures [58] using an impulse response function [59]. Second, the determined anthropogenic warming and the cumulative CO<sub>2</sub>-fe emissions (sum of CO<sub>2</sub> emissions from fossil fuels and land use change and CO<sub>2</sub>-fe from non-CO<sub>2</sub> radiative agents [3]) are used to determine the transient climate response to cumulative CO<sub>2</sub>-fe emissions (TCRE) [2, 3, 5, 8]. The TCRE then allows to estimate the remaining allowable emission budget (REB) of CO<sub>2</sub>-fe before the chosen temperature target is reached. In the third step, the CO<sub>2</sub>-fe in the REB are distributed over the next decades so that an overshoot in temperature is tried to be avoided and that year-to-year changes in CO<sub>2</sub>-fe emission reductions remain as small as possible. A detailed explanation of the AERA is provided by Terhaar *et al* [53].

### 2.2. Bern3D-LPX

Bern-3D-LPX is an Earth system model of intermediate complexity that simulates dynamically the

physics, chemistry, and biology of the land biosphere, the ocean, and sea ice, as well as their coupling to the atmosphere [60, 61]. The model is used at nine different setups that cover TCRES from 1.35 °C (EgC)<sup>-1</sup> to 2.16 °C (EgC)<sup>-1</sup>, which resembles the CMIP6 TCRES range of 1.32 °C–2.30 °C (EgC)<sup>-1</sup> [62] and the observation-constrained range of 1.3 °C–2.3 °C (EgC)<sup>-1</sup> [50] (EgC = 1000 PgC = 10<sup>18</sup> gC). The range of TCRES is obtained by combinations of three different ocean diapycnal mixing parameters ( $3 \times 10^{-5}$ ,  $2 \times 10^{-5}$ ,  $1 \times 10^{-5}$  m<sup>2</sup> s<sup>-1</sup>) and three different climate feedback parameters (-0.1, -0.5, -1.0 Wm<sup>-2</sup> K<sup>-1</sup>) that account for feedbacks in the Earth system that are not explicitly or potentially not correctly simulated by Bern3D-LPX. These setups were chosen as their range of ECSs from 2.3 to 4.6 °C covers the 5%–95% likelihood range of the latest ECS assessment based on multiple lines of evidence [63] and because the ocean mixing parameters result in a circulation that represents observed distributions of CFCs, O<sub>2</sub>, or Δ<sup>14</sup>C [61, 64].

### 2.3. Simulations and non-CO<sub>2</sub> radiative agents

The simulations with Bern3D-LPX start in 1765 and are until 2025 all prescribed with the same CO<sub>2</sub> emissions, non-CO<sub>2</sub> radiative forcing, and land use area change. CO<sub>2</sub> emissions are from the Global Carbon Budget until 2020 [65] and develop from 2021 to 2025 proportionally to the national determined contributions (NDC) as quantified by the Climate Action Tracker [66]. Non-CO<sub>2</sub> radiative forcing is based on the RCP database until 2000 [67–71] and from 2000 to 2025 on the most recent assessment from chapter 7 in the IPCC AR6 WG1 [72] report using SSP2-4.5 as an extension of the historical period after 2014 [44] to better reflect historic CH<sub>4</sub> and N<sub>2</sub>O emissions over the last years. Land-use change is prescribed from 1850 to 2100 based on SSP1-2.6 [73] and associated emissions are dynamically calculated by Bern3D-LPX. SSP1-2.6 was chosen for land-use change as CMIP simulations following this scenario result in temperature are on average between 1.5 °C and 2.0 °C [47], the temperature targets that are closest to the aims of the Paris Agreement to limit warming well below 2 °C and to pursue efforts to reduce it to 1.5 °C [1]. Volcanic radiative forcing is based on the Ice-core Volcanic Index 2 [74, 75] until 2000 and zero afterwards.

From 2025 to 2300, the emissions of CO<sub>2</sub>, N<sub>2</sub>O, CH<sub>4</sub>, CO, NO<sub>x</sub>, and VOC as well as trajectories of other non-CO<sub>2</sub> radiative agents, such as aerosols, evolve dynamically to match the prescribed CO<sub>2</sub>-fe emission curve, which is updated every five years. The AERA is first applied in 2025 and then every five years to mimic the stock take process foreseen in the Paris Agreement that includes a new submission of world-wide NDCs every five years with the next NDC submission being in 2025. The emissions of

N<sub>2</sub>O, CH<sub>4</sub>, CO, NO<sub>x</sub>, and VOC are used by a reduced form atmospheric chemistry model to calculate their respective atmospheric concentrations and the associated radiative forcing and CO<sub>2</sub>-fe emissions. A detailed explanation of the reduced atmospheric chemistry model and parameters is provided by Terhaar *et al* [53]. The ozone forcing and the aerosol forcing in the atmospheric chemistry model was here changed to 0.47 Wm<sup>-2</sup> and -1.06 Wm<sup>-2</sup> in 2019, respectively, to match the non-CO<sub>2</sub> radiative forcing from the IPCC AR6 WG1 report [72].

As many combinations of the different GHGs and radiative agents exist that would lead to the same prescribed CO<sub>2</sub>-fe emission curve, prior assumptions must be made for the evolution of the non-CO<sub>2</sub> radiative agents. Three sets of simulations were made to represent a wide range of future choices (supplementary table 1). In the first set of simulations, called ‘baseline’, CH<sub>4</sub> and N<sub>2</sub>O emissions evolve after 2020 according to SSP2-4.5, under which global warming will likely be limited to 2 °C warming [76], and CH<sub>4</sub> and N<sub>2</sub>O emissions are constant from 2100 onwards (supplementary figure 1). Although SSP1-2.6 represents the scenario that results in temperatures closest to the Paris Agreement targets (see above), we chose SSP2-4.5 to provide a set of simulations where CO<sub>2</sub> reductions are relatively higher so that the three sets of simulations span a range of CO<sub>2</sub> emissions. In addition, the aerosol radiative forcing decreases exponentially (80% with a lifetime of 100 years, and 20% with a lifetime of 50 years). CO<sub>2</sub> emissions evolve dynamically so that the total CO<sub>2</sub>-fe emission match the AERA-prescribed CO<sub>2</sub>-fe emissions. In the second set of simulations, called ‘high-CO<sub>2</sub>’, aerosols also decrease exponentially as in the ‘baseline’ simulations and CH<sub>4</sub> and N<sub>2</sub>O emissions evolve parallel to CO<sub>2</sub> emissions. The parallel evolution causes CH<sub>4</sub> and N<sub>2</sub>O emissions to decrease faster than under SSP2-4.5 and result accordingly in smaller CO<sub>2</sub>-fe emissions from CH<sub>4</sub> to N<sub>2</sub>O. Reductions in CO<sub>2</sub> emissions can therefore be weaker to still equal the same CO<sub>2</sub>-fe emission than in the baseline simulation, which yields comparatively higher CO<sub>2</sub> emissions. In the third set of simulation, called ‘constant aerosol’, CO<sub>2</sub>, CH<sub>4</sub>, and N<sub>2</sub>O emissions also evolve proportionally but the aerosol radiative forcing remains at 2025 levels. Therefore, even less stringent CO<sub>2</sub> emission reductions are necessary in this set of simulations to reach the temperature targets and CO<sub>2</sub> emissions and, in turn, atmospheric CO<sub>2</sub> can remain higher than in the ‘baseline’ and ‘high-CO<sub>2</sub>’ simulations. Land-use change remains unchanged across all simulations.

Throughout the manuscript, we focus on the ‘baseline’ and ‘high-CO<sub>2</sub>’ simulations that rely only on emission reductions, which are the only sustainable to reach a prescribed temperature target [77]. As opposed to these mitigation scenarios, the ‘constant aerosol’ simulations also rely on strong aerosol injection via solar radiation modification to

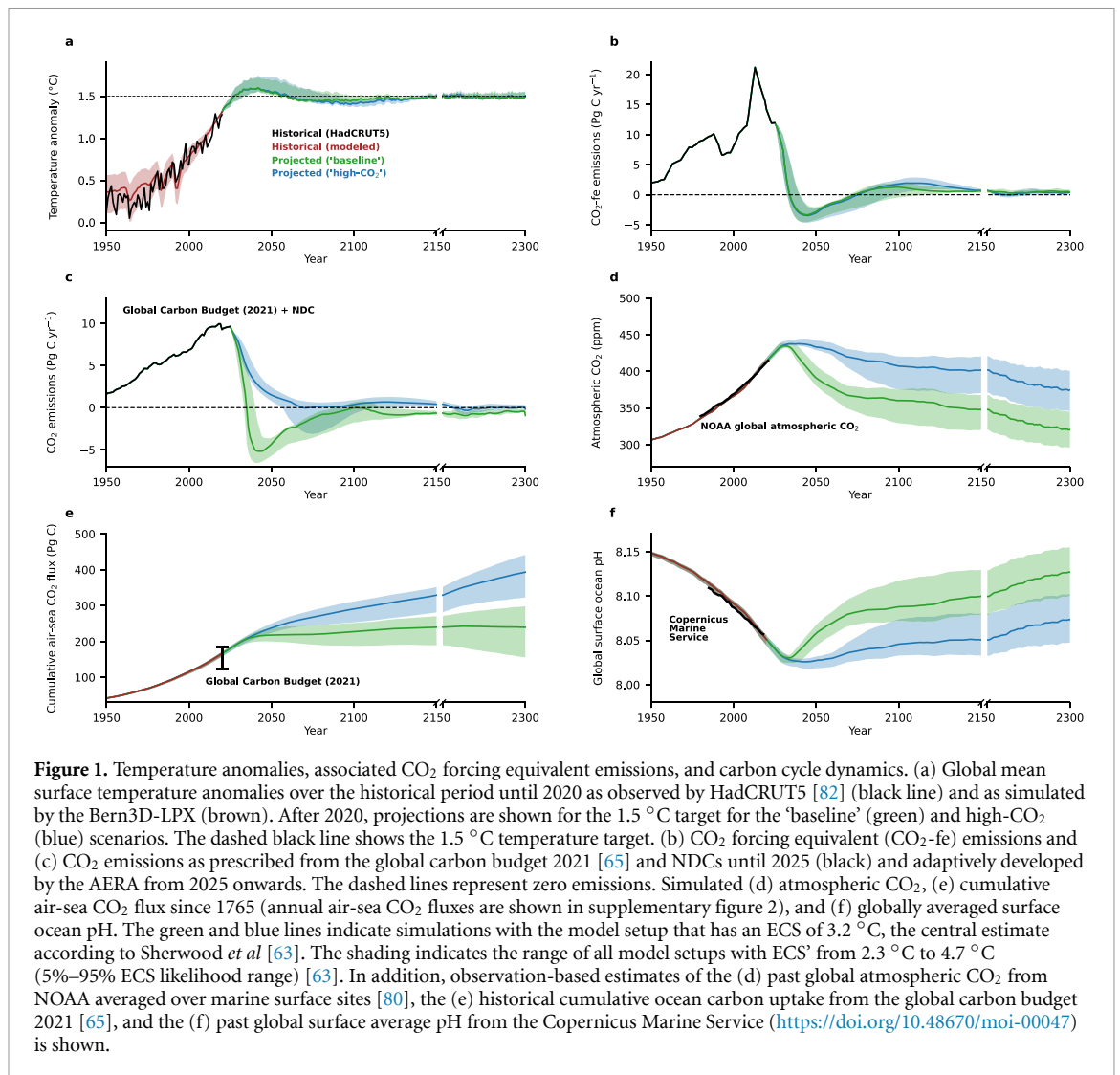


**Figure 1.** Temperature anomalies, associated  $\text{CO}_2$  forcing equivalent emissions, and carbon cycle dynamics. (a) Global mean surface temperature anomalies over the historical period until 2020 as observed by HadCRUT5 [82] (black line) and as simulated by the Bern3D-LPX (brown). After 2020, projections are shown for the  $1.5^\circ\text{C}$  target for the ‘baseline’ (green) and high- $\text{CO}_2$  (blue) scenarios. The dashed black line shows the  $1.5^\circ\text{C}$  temperature target. (b)  $\text{CO}_2$  forcing equivalent ( $\text{CO}_2\text{-fe}$ ) emissions and (c)  $\text{CO}_2$  emissions as prescribed from the global carbon budget 2021 [65] and NDCs until 2025 (black) and adaptively developed by the AERA from 2025 onwards. The dashed lines represent zero emissions. Simulated (d) atmospheric  $\text{CO}_2$ , (e) cumulative air-sea  $\text{CO}_2$  flux since 1765 (annual air-sea  $\text{CO}_2$  fluxes are shown in supplementary figure 2), and (f) globally averaged surface ocean pH. The green and blue lines indicate simulations with the model setup that has an ECS’ of  $3.2^\circ\text{C}$ , the central estimate according to Sherwood *et al* [63]. The shading indicates the range of all model setups with ECS’ from  $2.3^\circ\text{C}$  to  $4.7^\circ\text{C}$  (5%–95% ECS likelihood range) [63]. In addition, observation-based estimates of the (d) past global atmospheric  $\text{CO}_2$  from NOAA averaged over marine surface sites [80], the (e) historical cumulative ocean carbon uptake from the global carbon budget 2021 [65], and the (f) past global surface average pH from the Copernicus Marine Service (<https://doi.org/10.48670/moi-00047>) is shown.

keep the aerosol forcing constant. Solar radiation modification is only an emergency solution as it comes with high risks, e.g. an abrupt rise in temperatures if the solar radiation modification should fail in the future for technical or political reasons [78], further commitments and unintended side effects like shifting monsoon patterns, changes in meridional temperature gradients, atmospheric and oceanic circulation, and the modes of climate variability [79]. By presenting solar radiation modification briefly in the main manuscript and more detailed in the Supplementary Material, we transparently show all theoretical options but focus on the sustainable and more likely options.

In all simulation,  $\text{CH}_4$  and  $\text{N}_2\text{O}$  emissions have lower limits of  $30\text{ Tg CH}_4\text{ yr}^{-1}$  and  $5.3\text{ Tg N}_2\text{O yr}^{-1}$  due to non-abatable emissions in agriculture and livestock sectors. Simulations for the three set of simulations were made for four temperature targets of  $1.5^\circ\text{C}$ ,  $2.0^\circ\text{C}$ ,  $2.5^\circ\text{C}$ , and  $3.0^\circ\text{C}$  with each of the nine setups of Bern3D-LPX representing ECS’ from  $2.3^\circ\text{C}$  to  $4.7^\circ\text{C}$ , resulting in 108 simulations (3 set of simulations  $\times$  4 temperature targets  $\times$  9 Bern3D-LPX

setups). As Bern3D-LPX underestimates the inter-annual variability, each of these 108 setups was made with eight temporally varying superimposed inter-annual surface atmospheric temperature variabilities that are derived from observations [53] and hence yield 864 simulations in total (3 set of simulations  $\times$  4 temperature targets  $\times$  9 Bern3D-LPX setups  $\times$  8 temperature variabilities; supplementary table 1). The presented simulation results are openly available [83].

As all setups with different ECS simulate a different historical warming until 2020 compared to the 1850–1900 period ( $0.83^\circ\text{C}$ – $1.39^\circ\text{C}$ ), the remaining emissions and increases in atmospheric  $\text{CO}_2$  until a chosen temperature target is reached depends sensitively on this past warming. To remove this uncertainty, the temperature target is always defined relative to the observation-based anthropogenic warming in year 2020, which is estimated to be  $1.23 \pm 0.20^\circ\text{C}$  [53]. For the  $1.5^\circ\text{C}$  target, this means that an allowable warming of  $0.27^\circ\text{C}$  remains. This allowable warming is then added to the anthropogenic warming in each setup. This  $\Delta$ -approach is the same that is regularly

used for ocean acidification studies where different models have difficulties to simulate the baseline biogeochemistry in the interior ocean at present [23, 37, 39, 40].

### 3. The carbon cycle and ocean acidification in a stabilized 1.5 °C world

#### 3.1. Uncertainty from the transient climate response to cumulative carbon emissions

The simulated historical temperature anomaly with respect to 1850–1900 under prescribed CO<sub>2</sub> emissions increases at a similar pace as the observed temperature over all nine model setups ( $\pm 0.25$  °C), despite varying climate sensitivities and ocean carbon sink strengths (figure 1(a)). All model setups do not only capture the historical temperature trajectory, but also the observed trajectory of atmospheric CO<sub>2</sub> [80] (figure 1(d)), the observation-based estimate of the cumulative ocean carbon uptake [65] (figure 1(e)), and the globally averaged pH over the last decades (figure 1(f)).

After the AERA is switched on in 2025, all trajectories converge by 2150 within  $\pm 0.05$  °C to the prescribed 1.5 °C temperature target because fossil fuel CO<sub>2</sub> emissions evolve freely so that the combined CO<sub>2</sub>-fe emissions from fossil fuels, land use change, and non-CO<sub>2</sub> radiative agents match the prescribed CO<sub>2</sub>-fe emissions by the AERA. The total CO<sub>2</sub>-fe emissions from 2021 to 2150 that allow to meet the 1.5° target vary from  $-59$  Pg C to  $+203$  Pg C (range of nine setups after averaging over all eight realizations with varying inter-annual superimposed variability) under the ‘baseline’ scenario (figure 1(b)). The uncertainty ranges ( $-35$  Pg C to  $+239$  Pg C under the ‘high-CO<sub>2</sub>’ scenario;  $-27$  Pg C to  $+255$  Pg C under the ‘constant aerosol’ scenario) differ between the three scenarios due to the good but imperfect transformation of non-CO<sub>2</sub> radiative forcing to CO<sub>2</sub>-fe emissions. In simulations with the AERA that converge to a temperature target, the uncertainty from the TCRE transfers into the CO<sub>2</sub>-fe budget, whereas traditional projections used in the IPCC reports [47] based on shared socioeconomic pathways (SSPs) [44, 45, 81] have an inter-model temperature range for a given CO<sub>2</sub>-fe trajectory (for example, the 5%–95% range for global warming in 2100 under SSP1-2.6 is 1.3 °C–2.8 °C) [47].

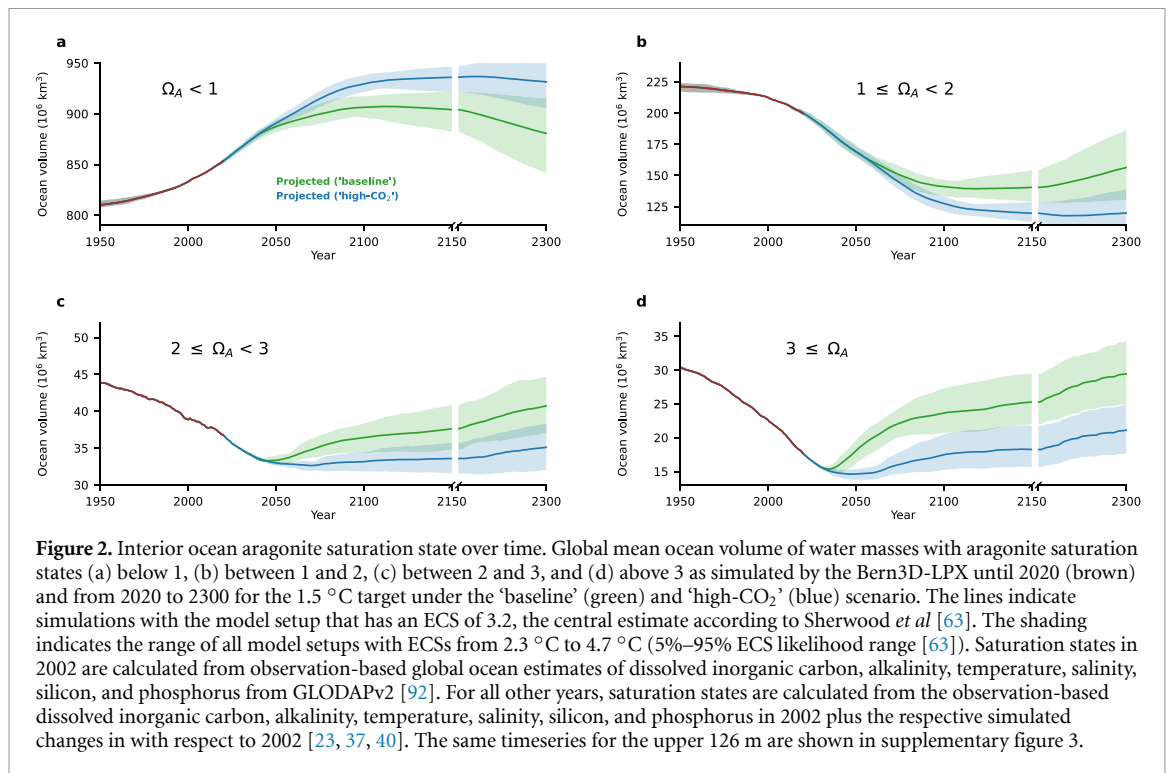
The range of cumulative CO<sub>2</sub>-fe emissions from 2021 to 2150 that allow to meet the 1.5 °C target ( $-59$  Pg C to  $+203$  Pg C for the ‘baseline’ scenario) propagates directly into different fossil fuel CO<sub>2</sub> emission trajectories. The remaining allowable fossil fuel CO<sub>2</sub> emissions depend on AERA derived CO<sub>2</sub>-fe emissions and the non-CO<sub>2</sub> emissions and the CO<sub>2</sub> emissions from land-use change. In the ‘baseline’ scenario, CH<sub>4</sub> and N<sub>2</sub>O emissions and aerosols follow prescribed trajectories, resulting in CO<sub>2</sub>-fe emissions

of all non-CO<sub>2</sub> radiative agents from 2021 to 2150 of 160 Pg C and land-use change emissions of 17 Pg C. Therefore, the remaining allowable fossil-fuel CO<sub>2</sub> emissions from 2021 to 2150 under this scenario range from  $-236$  Pg C to  $+25$  Pg C (figure 1(c)).

The range of CO<sub>2</sub> emission trajectories affects the projected atmospheric CO<sub>2</sub> and the rates and magnitude of ocean carbon uptake (figures 1(d) and (e), supplementary figure S2). By 2150, possible atmospheric CO<sub>2</sub> in a 1.5 °C world under the ‘baseline’ scenario range from 320 ppm to 368 ppm after having peaked at 433–439 ppm between 2030 and 2035, and the cumulative ocean carbon sink from 1765 to 2150 varies from 190 Pg C to 271 Pg C. In comparison, the SSPs that are used by the IPCC have by definition no uncertainty in the future atmospheric CO<sub>2</sub> as atmospheric CO<sub>2</sub> is prescribed as a boundary condition. While the uncertainty of the atmospheric CO<sub>2</sub> in 2100 is by definition non-existent, the range of the cumulative carbon sink is also smaller when atmospheric CO<sub>2</sub> is prescribed, for example 274–332 Pg C for SSP1-2.6 across the CMIP6 ensemble [56]. Thus, when CO<sub>2</sub> emissions evolve freely to converge to a temperature target, the range of the future sink is  $\sim 40\%$  larger than under fixed atmospheric CO<sub>2</sub>.

The wide range of possible atmospheric CO<sub>2</sub> translates into different surface ocean pH projections. At the ocean surface changes in pH are almost entirely driven by changing dissolved inorganic carbon [57], which in turn closely follows the changes in atmospheric CO<sub>2</sub> due to the air-sea CO<sub>2</sub> flux that tends to equilibrate differences in CO<sub>2</sub> partial pressure between the atmosphere and ocean. Hence, the projected atmospheric CO<sub>2</sub> range from 320 ppm to 368 ppm in 2150 results in an almost perfectly anti-correlated projected range in surface ocean pH from 8.079 to 8.129 (after a minimum of 8.024–8.033 between 2031 and 2037) (figures 1(d)–(f)). This range is an order of magnitude larger than the projected standard deviation in projected ocean surface pH of  $\pm 0.002$  under SSP1-2.6 in 2100 [19]. Furthermore, the annually averaged surface area that is projected to have saturation states of aragonite—a mineral form of calcium carbonate produced by marine organisms—below one remains almost non-existent ( $< 10^6$  km<sup>2</sup>) due to the rapidly decreasing CO<sub>2</sub> emissions. However, saturation states may still drop below one on diurnal [84, 85] or seasonal [31, 86] timescales or in the 126 m below the surface (figure 3(f), supplementary figure 3), where calcifying organisms vertically migrate [87].

As opposed to surface ocean acidification, long-term ocean acidification below the surface depends not only on the increasing surface ocean dissolved inorganic carbon but also on the quantity of additional dissolved inorganic carbon at the ocean surface that is transported below the ocean surface [31, 37, 39, 40, 56, 88] and distributed within the ocean



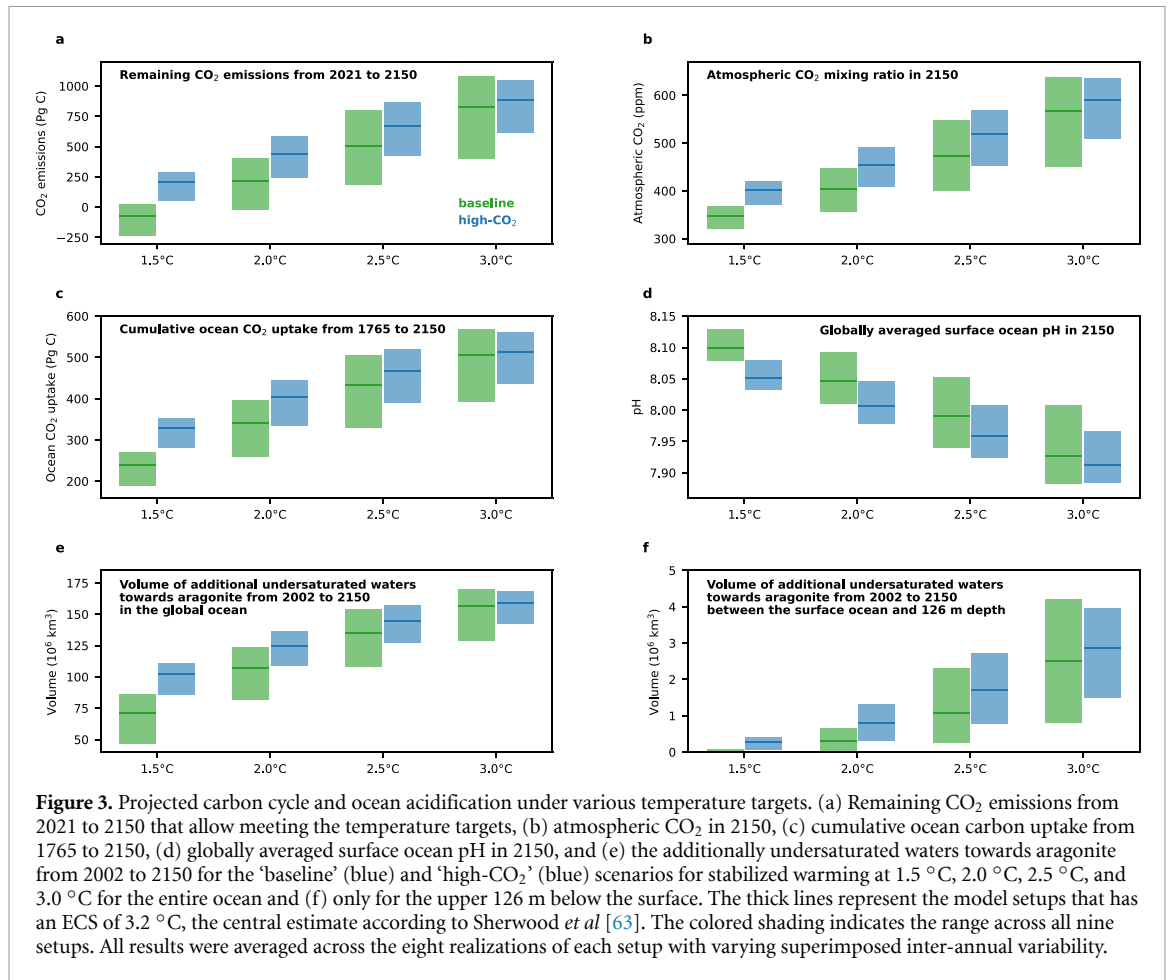
[42, 89]. The decrease in the global ocean volume that is projected to remain saturated towards aragonite ( $\Omega_A > 1$ ) from 2002 to 2150 ranges from 47 to  $86 \times 10^6 \text{ km}^3$  (17%–32% of supersaturated volume in 2002) (figure 2(a)), with the central estimate (setup with ECS = 3.2 °C) being  $71 \times 10^6 \text{ km}^3$  (26%) and the standard deviation across all nine setups being  $12 \times 10^6 \text{ km}^3$  (4%). Similarly, the range in volumes changes with  $\Omega_A$  between 1 and 2, 2 and 3, and above 3 vary strongly across the different model setups. Under prescribed atmospheric CO<sub>2</sub> in SSP1-2.6, the simulated decrease in volume that is projected to remain saturated towards aragonite ( $\Omega_A > 1$ ) in 2100 is  $89 \pm 6 \times 10^6 \text{ km}^3$  [56]. Thus, the uncertainty of future interior ocean acidification rates under a prescribed temperature target when using the AERA is around twice as large as under prescribed atmospheric CO<sub>2</sub>. The difference in uncertainty under prescribed temperature targets and prescribed atmospheric CO<sub>2</sub> is smaller in the ocean interior (factor 2) than at the ocean surface (factor 10), because most water masses are not in direct contact with the atmosphere so that the differences in simulated ocean circulation and deep-water formation affects both kinds of simulations [37, 39, 40, 56, 90, 91].

### 3.2. Uncertainty from the choice of reductions of non-CO<sub>2</sub> radiative agents

The evolution of non-CO<sub>2</sub> radiative forcing agents does not influence the temperature and CO<sub>2</sub>-fe trajectory (figures 1(a) and (b)) but limits, for a given temperature target, the range of possible future trajectories of CO<sub>2</sub> emissions, atmospheric CO<sub>2</sub>, ocean carbon uptake, surface ocean pH, and interior ocean

aragonite saturation states (figures 1(c)–(f) and 2). Under the ‘baseline’ scenario, non-CO<sub>2</sub> radiative agents are prescribed following SSP2-4.5 and the radiative forcing of major non-CO<sub>2</sub> radiative agents (N<sub>2</sub>O, CH<sub>4</sub>, and aerosols) under SSP2-4.5 do not get strongly reduced. Thus, the reduction in CO<sub>2</sub>-fe emissions as prescribed by the AERA is achieved via reductions in CO<sub>2</sub> emissions. As opposed to the ‘baseline’ scenario, the radiative forcing or emissions of the major non-CO<sub>2</sub> radiative agents are reduced strongly under the ‘high-CO<sub>2</sub>’ scenario so that CO<sub>2</sub> emissions remain higher from 2025 to 2075, yielding a remaining CO<sub>2</sub> budget from 2021 to 2150 of 54–286 Pg C, significantly larger than the –236 Pg C to +25 Pg C range under the ‘baseline’ scenario. As CO<sub>2</sub> emissions are larger under the ‘high-CO<sub>2</sub>’ scenario, so are atmospheric CO<sub>2</sub> (371–420 ppm in 2150 after having peaked at 436–445 ppm between 2034 and 2043), and the cumulative carbon uptake by the ocean (281–352 Pg C in 2150).

The larger atmospheric CO<sub>2</sub> in the ‘high-CO<sub>2</sub>’ scenario and the larger cumulative carbon uptake by the ocean result in higher ocean acidification. The range of projected surface ocean pH across the nine different model setups with stronger reduction in non-CO<sub>2</sub> radiative agents is 8.033–8.080 in 2150 (after a minimum of 8.018–8.029 between 2042 and 2047) (figures 1(d)–(f)). The decrease in volume that is projected to remain saturated towards aragonite ( $\Omega_A > 1$ ) in 2150 under the ‘high-CO<sub>2</sub>’ scenario ranges from 86 to  $111 \times 10^6 \text{ km}^3$  (31%–41%) (figure 2(a)). Overall, the choice of non-CO<sub>2</sub> radiative forcing agents hence increases the possible range of ocean acidification rates in a 1.5 °C world by a



factor of two and makes the uncertainty about the future ocean acidification rates in a 1.5 °C world thus even larger than it already was due to the different TCRE’s (see above). The entire range of globally averaged surface ocean pH under both scenarios of 0.096 is thus as large as the difference in surface ocean pH between SSP1-2.6 (warming of 1.3 °C–2.8 °C [47]) and SSP2-4.5 (warming of 2.1 °C–4.0 °C) and ~50 times as large as the inter-model difference for each scenario across the range of CMIP6 Earth system models [19].

In addition to the ‘high-CO<sub>2</sub>’ scenario, the ‘constant aerosol’ scenario allows to assess a potential future in which the necessary GHG reductions are compensated by continuing aerosol emissions so that the cooling effect of aerosols in the atmosphere does not reduce over the 21st century. In that scenario, the CO<sub>2</sub> emissions can remain even higher, yielding higher atmospheric CO<sub>2</sub> in 2150 (411–465 ppm), higher ocean cumulative CO<sub>2</sub> uptake from 1765 to 2150 (335–405 Pg C), and much more severe ocean acidification with globally averaged pH values in 2150 ranging from 7.998 to 8.045 (supplementary figure 4). This example demonstrates the importance of multiple climate targets [17] in addition to temperature targets to reduce the damaging effect of anthropogenic emissions on Earth ecosystems.

#### 4. The carbon cycle and ocean acidification if global warming permanently exceeds the temperature targets of the Paris Agreements

The Paris Agreement aims at limiting global warming well below 2 °C and reducing it to 1.5 °C [1]. However, recent carbon and non-CO<sub>2</sub> GHG emissions suggest that this target may not be met [66, 93]. Hence, it is important to quantify the effect of different warming levels that permanently overshoot the Paris Agreement temperature goals on the carbon cycle and ocean acidification. In this section, the projected atmospheric CO<sub>2</sub>, ocean carbon uptake, surface ocean pH, and interior ocean  $\Omega_A$  are quantified for a 2.0 °C, 2.5 °C, and 3.0 °C target (figure 3, supplementary table 2) although many other targets would be possible.

With increasing warming, the range across setups increases as the transient climate response to cumulative emissions (TCRE) leads to a higher range in the remaining emission budget for a higher temperature target. In 2150, when the temperature stabilizes in these simulations, the higher range in the remaining emission results in large uncertainty ranges in past cumulative CO<sub>2</sub> emissions and ocean carbon uptake, as well as large ranges in atmospheric CO<sub>2</sub>, surface



ocean pH, and the volume of water undersaturated towards aragonite are simulated across the different model setups. These ranges even overlap for different temperature targets. Under the 'baseline' scenario, even the projections for the 2.0 °C and 3.0 °C target almost overlap. When adding uncertainties from the choice of the non-CO<sub>2</sub> emissions, the projections of the 2.0 °C and 3.0 °C targets overlap strongly. Furthermore, the differences between the projections of the carbon cycle between the 'baseline' and 'high-CO<sub>2</sub>' are reduced under higher temperature targets because non-CO<sub>2</sub> emissions under the 'high-CO<sub>2</sub>' are proportional to CO<sub>2</sub> emissions. As CO<sub>2</sub> emissions remain higher for a warmer temperature target so are the emissions of non-CO<sub>2</sub> radiative agents, which remain hence closer to the prescribed emissions of non-CO<sub>2</sub> radiative agents under the 'baseline' scenario.

Overall, the comparison demonstrates the large uncertainties of the carbon cycle projections under prescribed temperature targets, which are not apparent under usual projections by Earth system models under RCPs or SSPs with prescribed trajectories of atmospheric CO<sub>2</sub> and non-CO<sub>2</sub> radiative agents.

## 5. Conclusion

The simulations with the AERA allow assessing the so-far largely unknown uncertainties of the ocean carbon cycle and ocean acidification under prescribed temperature targets. Until now, future ocean acidification was assessed by the IPCC [33] and other studies [18, 19] using scenarios with prescribed atmospheric CO<sub>2</sub> trajectories [18, 19, 33] and only few studies assessed uncertainties in acidification metrics by prescribing, adapting, or remapping carbon emissions [49–52]. The uncertainties for global and regional ocean acidification projections under prescribed atmospheric CO<sub>2</sub> trajectories were reduced with great efforts by understanding differences between the different Earth system models [37, 39, 40, 56]. However, here we show that the uncertainties stemming from the TCRE, which is determined by the Earth's warming response to GHGs, e.g. ECS, and ocean carbon uptake, are twice as large to a magnitude larger than the inter-model differences in the usual projections.

The here provided simulations are made with an Earth system model of intermediate complexity and provide robust projections of the globally or basin-wide averaged projections. For projections of ocean acidification on a regional scale like the Gulf of Alaska [94], the Eastern Boundary upwelling systems [95, 96], the Arctic Ocean [37, 40], or the Southern Ocean [39, 89], state-of-the-art Earth system models representing small scale circulation [42, 97–99] would need to be run with the AERA in the future.

The difference in the projected future of the ocean carbon uptake and ocean acidification also highlights

the importance of the choice of emission reductions between CO<sub>2</sub> and non-CO<sub>2</sub> emissions for the ocean ecosystems that are vulnerable to ocean acidification. While many different combinations of reductions in CO<sub>2</sub> and non-CO<sub>2</sub> emissions allow reaching a given temperature target, these different combinations may affect ecosystems vulnerable to ocean acidification in very different ways. In the case of ocean acidification, the same amount of CO<sub>2</sub>-fe emissions in form of CO<sub>2</sub> emissions is more harmful to the ocean than in form of N<sub>2</sub>O or CH<sub>4</sub> emissions. Moreover, the possible implementation of solar radiation modification, e.g. via continuing aerosol emissions, to limit global warming to 1.5 °C would still cause high ocean acidification rates. Hence, when agreeing on climate targets policy makers should not only focus on warming levels [1], but also on other climate targets [17].

## Data availability statement

The data that support the findings of this study are openly available at the following URL/DOI: <https://doi.org/10.17882/92735>.

## Acknowledgments

This work was funded by the European Union's Horizon 2020 research and innovation program under Grant Agreement No. 821003 (Project 4C, Climate–Carbon Interactions in the Current Century) (Jens Terhaar, Thomas L Frölicher, Fortunat Joos) No. 820989 (Project COMFORT, Our common future ocean in the Earth system-quantifying coupled cycles of carbon, oxygen and nutrients for determining and achieving safe operating spaces with respect to tipping points) (Thomas L Frölicher, Fortunat Joos), and No. 101003687 (Project PROVIDE, Paris Agreement Overshooting) (Thomas L. Frölicher) as well as by Woods Hole Oceanographic Institution Postdoctoral Scholar Program (Jens Terhaar), and the Swiss National Science Foundation under Grant PP00P2\_198897 (Thomas L Frölicher) and Grant #200020\_200511 (Jens Terhaar, Fortunat Joos). This study has been conducted using E.U. Copernicus Marine Service Information; <https://doi.org/10.48670/moi-00047>. The work reflects only the authors' view; the European Commission and their executive agency are not responsible for any use that may be made of the information the work contains.

## Author contributions

J T, T L F, and F J are responsible for conceptualization and methodology. J T made the simulations, analyses, visualization, and wrote the original draft. T L F and F J were responsible for funding acquisition. T L F and F J were responsible for project administration. J T,

T L F, and F J were responsible for writing, review, and editing.

### Conflict of interest

The contact author has declared that none of the authors has any competing interests.

### ORCID iDs

Jens Terhaar  <https://orcid.org/0000-0001-9377-415X>

Thomas L Frölicher  <https://orcid.org/0000-0003-2348-7854>

Fortunat Joos  <https://orcid.org/0000-0002-9483-6030>

### References

- [1] UNFCCC 2015 United Nations Paris Agreement. Report of the conference of the parties to the united nations framework convention on climate change (Paris)
- [2] Jenkins S, Millar R J, Leach N and Allen M R 2018 Framing climate goals in terms of cumulative CO<sub>2</sub>-forcing-equivalent emissions *Geophys. Res. Lett.* **45** 2795–804
- [3] Smith M A, Cain M and Allen M R 2021 Further improvement of warming-equivalent emissions calculation *npj Clim. Atmos. Sci* **4** 19
- [4] Matthews H D and Caldeira K 2008 Stabilizing climate requires near-zero emissions *Geophys. Res. Lett.* **35** L04705
- [5] Matthews H D, Gillett N P, Stott P A and Zickfeld K 2009 The proportionality of global warming to cumulative carbon emissions *Nature* **459** 829–32
- [6] Allen M R, Frame D J, Huntingford C, Jones C D, Lowe J A, Meinshausen M and Meinshausen N 2009 Warming caused by cumulative carbon emissions towards the trillionth tonne *Nature* **458** 1163–6
- [7] MacDougall A H et al 2020 Is there warming in the pipeline? A multi-model analysis of the zero emissions commitment from CO<sub>2</sub> *Biogeosciences* **17** 2987–3016
- [8] Zickfeld K, Eby M, Matthews H D and Weaver A J 2009 Setting cumulative emissions targets to reduce the risk of dangerous climate change *Proc. Natl Acad. Sci.* **106** 16129
- [9] Zickfeld K, MacDougall A H and Matthews H D 2016 On the proportionality between global temperature change and cumulative CO<sub>2</sub> emissions during periods of net negative CO<sub>2</sub> emissions *Environ. Res. Lett.* **11** 055006
- [10] Allen M R, Shine K P, Fuglestedt J S, Millar R J, Cain M, Frame D J and Macey A H 2018 A solution to the misrepresentations of CO<sub>2</sub>-equivalent emissions of short-lived climate pollutants under ambitious mitigation *npj Clim. Atmos. Sci* **1** 16
- [11] Damon Matthews H, Tokarska K B, Rogelj J, Smith C J, MacDougall A H, Hausteine K, Mengis N, Sippel S, Forster P M and Knutti R 2021 An integrated approach to quantifying uncertainties in the remaining carbon budget *Commun. Earth Environ.* **2** 7
- [12] Rogelj J, Forster P M, Kriegler E, Smith C J and Séférian R 2019 Estimating and tracking the remaining carbon budget for stringent climate targets *Nature* **571** 335–42
- [13] Tokarska K B, Zickfeld K and Rogelj J 2019 Path independence of carbon budgets when meeting a stringent global mean temperature target after an overshoot *Earth's Future* **7** 1283–95
- [14] Jones C D and Friedlingstein P 2020 Quantifying process-level uncertainty contributions to TCRE and carbon budgets for meeting Paris Agreement climate targets *Environ. Res. Lett.* **15** 074019
- [15] Peters P G 2018 Beyond carbon budgets *Nat. Geosci.* **11** 378–80
- [16] Matthews H D et al 2020 Opportunities and challenges in using remaining carbon budgets to guide climate policy *Nat. Geosci.* **13** 769–79
- [17] Steinacher M, Joos F and Stocker T F 2013 Allowable carbon emissions lowered by multiple climate targets *Nature* **499** 197–201
- [18] Bopp L et al 2013 Multiple stressors of ocean ecosystems in the 21st century: projections with CMIP5 models *Biogeosciences* **10** 6225–45
- [19] Kwiatkowski L et al 2020 Twenty-first century ocean warming, acidification, deoxygenation, and upper-ocean nutrient and primary production decline from CMIP6 model projections *Biogeosciences* **17** 3439–70
- [20] Boyd P W and Brown C J 2015 Modes of interactions between environmental drivers and marine biota *Front. Mar. Sci.* **2** 9
- [21] Kroeker K J, Kordas R L, Crim R N and Singh G G 2010 Meta-analysis reveals negative yet variable effects of ocean acidification on marine organisms *Ecol. Lett.* **13** 1419–34
- [22] Doney S C, Busch D S, Cooley S R and Kroeker K J 2020 The impacts of ocean acidification on marine ecosystems and reliant human communities *Annu. Rev. Environ. Resour.* **45** 83–112
- [23] Orr J C 2005 et al Anthropogenic ocean acidification over the twenty-first century and its impact on calcifying organisms *Nature* **437** 681–6
- [24] Gattuso J-P and Hansson L 2011 *Ocean Acidification* (Oxford: Oxford University Press) (<https://doi.org/10.1093/oso/9780199591091.001.0001>)
- [25] Kroeker K J, Kordas R L, Crim R, Hendriks I E, Ramajo L, Singh G S, Duarte C M and Gattuso J-P 2013 Impacts of ocean acidification on marine organisms: quantifying sensitivities and interaction with warming *Glob. Chang. Biol.* **19** 1884–96
- [26] Kawaguchi S, Ishida A, King R, Raymond B, Waller N, Constable A, Nicol S, Wakita M and Ishimatsu A 2013 Risk maps for Antarctic krill under projected Southern Ocean acidification *Nat. Clim. Change* **3** 843–7
- [27] Albright R et al 2016 Reversal of ocean acidification enhances net coral reef calcification *Nature* **531** 362–5
- [28] Fabry V J, Seibel B A, Feely R A and Orr J C 2008 Impacts of ocean acidification on marine fauna and ecosystem processes *ICES J. Mar. Sci.* **65** 414–32
- [29] AMAP 2013 *AMAP Assessment 2013: Arctic Ocean Acidification* (Oslo: Arctic Monitoring and Assessment Programme (AMAP)) (available at: [www.amap.no/documents/download/1577/inline](http://www.amap.no/documents/download/1577/inline))
- [30] Riebesell U, Gattuso J-P, Thingstad T F and Middelburg J J 2013 Preface “Arctic ocean acidification: pelagic ecosystem and biogeochemical responses during a mesocosm study” *Biogeosciences* **10** 5619–26
- [31] Steinacher M, Joos F, Frölicher T L, Plattner G-K and Doney S C 2009 Imminent ocean acidification in the Arctic projected with the NCAR global coupled carbon cycle-climate model *Biogeosciences* **6** 515–33
- [32] Orr J C, Kwiatkowski L and Pörtner H-O 2022 Arctic Ocean annual high in pCO<sub>2</sub> could shift from winter to summer *Nature* **610** 94–100
- [33] Canadell J G et al 2021 Global carbon and other biogeochemical cycles and feedbacks *Climate Change 2021: The Physical Science Basis: Contribution of Working Group I to the Sixth: Assessment Report of the Intergovernmental Panel on Climate Change* ed V Masson-Delmotte et al (Cambridge: Cambridge University Press) pp 673–816
- [34] Duarte C M, Hendriks I E, Moore T S, Olsen Y S, Steckbauer A, Ramajo L, Carstensen J, Trotter J A and McCulloch M 2013 Is ocean acidification an open-ocean syndrome? Understanding anthropogenic impacts on seawater pH *Estuaries Coast.* **36** 221–36
- [35] Tank S E, Raymond P A, Striegl R G, McClelland J W, Holmes R M, Fiske G J and Peterson B J 2012 A

- land-to-ocean perspective on the magnitude, source and implication of DIC flux from major Arctic rivers to the Arctic Ocean *Glob. Biogeochem. Cycles* **26** GB4018
- [36] Terhaar J, Orr J C, Ethé C, Regnier P and Bopp L 2019 Simulated Arctic Ocean response to doubling of riverine carbon and nutrient delivery *Glob. Biogeochem. Cycles* **33** 1048–70
- [37] Terhaar J, Torres O, Bourgeois T and Kwiatkowski L 2021 Arctic Ocean acidification over the 21st century co-driven by anthropogenic carbon increases and freshening in the CMIP6 model ensemble *Biogeosciences* **18** 2221–40
- [38] Woosley R J and Millero F J 2020 Freshening of the western Arctic negates anthropogenic carbon uptake potential *Limnol. Oceanogr.* **65** 1834–46
- [39] Terhaar J, Frölicher T and Joos F 2021 Southern Ocean anthropogenic carbon sink constrained by sea surface salinity *Sci. Adv.* **7** 5964–92
- [40] Terhaar J, Kwiatkowski L and Bopp L 2020 Emergent constraint on Arctic Ocean acidification in the twenty-first century *Nature* **582** 379–83
- [41] Chierici M and Fransson A 2009 Calcium carbonate saturation in the surface water of the Arctic Ocean: undersaturation in freshwater influenced shelves *Biogeosciences* **6** 2421–31
- [42] Terhaar J, Orr J C, Gehlen M, Ethé C and Bopp L 2019 Model constraints on the anthropogenic carbon budget of the Arctic Ocean *Biogeosciences* **16** 2343–67
- [43] Burger F A, John J G and Frölicher T L 2020 Increase in ocean acidity variability and extremes under increasing atmospheric CO<sub>2</sub> *Biogeosciences* **17** 4633–62
- [44] Riahi K et al 2017 The shared socioeconomic pathways and their energy, land use, and greenhouse gas emissions implications: an overview *Glob. Environ. Change* **42** 153–68
- [45] O'Neill B C et al 2016 The scenario model intercomparison project (ScenarioMIP) for CMIP6 *Geosci. Model. Dev.* **9** 3461–82
- [46] IPCC 2013 *Climate Change 2013: The Physical Science Basis. Contribution of Working Group I to the Fifth Assessment Report of the Intergovernmental Panel on Climate Change Summary for Policymakers Intergovernmental Panel On Climate Change* (Cambridge: Cambridge University Press) (<https://doi.org/10.1017/CBO9781107415324.004>)
- [47] IPCC 2021 *Climate Change 2021: the physical science basis Contribution of Working Group I to the Sixth Assessment Report of the Intergovernmental Panel on Climate Change Summary for Policymakers* (Cambridge: Cambridge University Press) (<https://doi.org/10.1017/9781009157896.001>)
- [48] Frölicher T L, Rodgers K B, Stock C A and Cheung W W L 2016 Sources of uncertainties in 21st century projections of potential ocean ecosystem stressors *Glob. Biogeochem. Cycles* **30** 1224–43
- [49] Joos F, Frölicher T L, Steinacher M and Plattner G-K 2011 Impact of climate change mitigation on ocean acidification projections *Ocean Acidification* ed J-P Gattuso and L Hansson (Oxford: Oxford University Press) pp 272–90
- [50] Steinacher M and Joos F 2016 Transient Earth system responses to cumulative carbon dioxide emissions: linearities, uncertainties, and probabilities in an observation-constrained model ensemble *Biogeosciences* **13** 1071–103
- [51] Goodwin P, Brown S, Haigh I D, Nicholls R J and Matter J M 2018 Adjusting mitigation pathways to stabilize climate at 1.5 °C and 2.0 °C rise in global temperatures to year 2300 *Earth's Future* **6** 601–15
- [52] Nicholls R J et al 2018 Stabilization of global temperature at 1.5 °C and 2.0 °C: implications for coastal areas *Phil. Trans. R. Soc. A.* **376** 20160448
- [53] Terhaar J, L F T, Aschwanden M T, Friedlingstein P and Joos F 2022 Adaptive emission reduction approach to reach any global warming target *Nat. Clim. Change* **12** 1136–42
- [54] Lienert S and Joos F 2018 A Bayesian ensemble data assimilation to constrain model parameters and land-use carbon emissions *Biogeosciences* **15** 2909–30
- [55] Roth R, Ritz S P and Joos F 2014 Burial-nutrient feedbacks amplify the sensitivity of atmospheric carbon dioxide to changes in organic matter remineralisation *Earth Syst. Dyn.* **5** 321–43
- [56] Terhaar J, Frölicher T L and Joos F 2022 Observation-constrained estimates of the global ocean carbon sink from Earth system models *Biogeosciences* **19** 4431–57
- [57] Burger F A, Terhaar J and Frölicher T L 2022 Compound marine heatwaves and ocean acidity extremes *Nat. Commun.* **13** 4722
- [58] Otto F E L, Frame D J, Otto A and Allen M R 2015 Embracing uncertainty in climate change policy *Nat. Clim. Change* **5** 917–20
- [59] Joos F et al 2013 Carbon dioxide and climate impulse response functions for the computation of greenhouse gas metrics: a multi-model analysis *Atmos. Chem. Phys.* **13** 2793–825
- [60] Ritz S P, Stocker T F and Joos F 2011 A coupled dynamical ocean–energy balance atmosphere model for paleoclimate studies *J. Clim.* **24** 349–75
- [61] Battaglia G and Joos F 2018 Marine N<sub>2</sub>O emissions from nitrification and denitrification constrained by modern observations and projected in multimillennial global warming simulations *Glob. Biogeochem. Cycles* **32** 92–121
- [62] Arora V K et al 2020 Carbon–concentration and carbon–climate feedbacks in CMIP6 models and their comparison to CMIP5 models *Biogeosciences* **17** 4173–222
- [63] Sherwood S C et al 2020 An assessment of Earth's climate sensitivity using multiple lines of evidence *Rev. Geophys.* **58** e2019RG000678
- [64] Battaglia G, Steinacher M and Joos F 2016 A probabilistic assessment of calcium carbonate export and dissolution in the modern ocean *Biogeosciences* **13** 2823–48
- [65] Friedlingstein P et al 2022 Global carbon budget 2021 *Earth Syst. Sci. Data* **14** 1917–2005
- [66] Ecofys, CA and PIK 2009 *Climate Action Tracker* (available at: <https://climateactiontracker.org/>)
- [67] Lamarque J-F et al 2010 Historical (1850–2000) gridded anthropogenic and biomass burning emissions of reactive gases and aerosols: methodology and application *Atmos. Chem. Phys.* **10** 7017–39
- [68] Smith S J, Pitcher H and Wigley T M L 2001 Global and regional anthropogenic sulfur dioxide emissions *Glob. Planet. Change* **29** 99–119
- [69] Bond T C, Bhardwaj E, Dong R, Jogani R, Jung S, Roden C, Streets D G and Trautmann N M 2007 Historical emissions of black and organic carbon aerosol from energy-related combustion, 1850–2000 *Glob. Biogeochem. Cycles* **21** GB2018
- [70] Eyring V, Isaksen I S A, Bernsten T, Collins W J, Corbett J J, Endresen O, Grainger R G, Moldanova J, Schlager H and Stevenson D S 2010 Transport impacts on atmosphere and climate: shipping *Atmos. Environ.* **44** 4735–71
- [71] Lee D S, Fahey D W, Forster P M, Newton P J, Wit R C N, Lim L L, Owen B and Sausen R 2009 Aviation and global climate change in the 21st century *Atmos. Environ.* **43** 3520–37
- [72] Forster P 2021 The Earth's energy budget, climate feedbacks, and climate sensitivity *Clim. Chang. 2021 Phys. Sci. Basis. Contrib. Work. Gr. I To Sixth Assess. Rep. Intergov. Panel Clim. Chang* ed V Masson-Delmotte et al (Cambridge: Cambridge University Press) pp 923–1054
- [73] Hurtt G C et al 2020 Harmonization of global land use change and management for the period 850–2100 (LUH2) for CMIP6 *Geosci. Model. Dev.* **13** 5425–64
- [74] Gao C, Robock A and Ammann C 2008 Volcanic forcing of climate over the past 1500 years: an improved ice core-based index for climate models *J. Geophys. Res. Atmos.* **113** D23111
- [75] Schmidt G A et al 2012 Climate forcing reconstructions for use in PMIP simulations of the last millennium (v1.1) *Geosci. Model. Dev.* **5** 185–91

- [76] Fricko O *et al* 2017 The marker quantification of the shared socioeconomic pathway 2: a middle-of-the-road scenario for the 21st century *Glob. Environ. Change* **42** 251–67
- [77] IPCC 2022 Climate Change 2022: mitigation of climate change *Contribution of Working Group III to the Sixth Assessment Report of the Intergovernmental Panel on Climate Change Summary for Policymakers* (Cambridge: Cambridge University Press) (<https://doi.org/10.1017/9781009157926.001>)
- [78] Robock A, Oman L and Stenchikov G L 2008 Regional climate responses to geoengineering with tropical and Arctic SO<sub>2</sub> injections *J. Geophys. Res. Atmos.* **113** D16101
- [79] National Academies of Sciences Engineering and Medicine 2021 *Reflecting Sunlight: Recommendations for Solar Geoengineering Research and Research Governance* (Washington, DC: The National Academies Press) (<https://doi.org/10.17226/25762>)
- [80] Dlugokencky E and Tans P Trends in atmospheric carbon dioxide (NOAA/GML) NOAA/GML (available at: <https://gml.noaa.gov/ccgg/trends/>)
- [81] van Vuuren D P *et al* 2017 Energy, land-use and greenhouse gas emissions trajectories under a green growth paradigm *Glob. Environ. Change* **42** 237–50
- [82] Morice C P, Kennedy J J, Rayner N A, Winn J P, Hogan E, Killick R E, Dunn R J H, Osborn T J, Jones P D and Simpson I R 2021 An updated assessment of near-surface temperature change from 1850: the HadCRUT5 data set *J. Geophys. Res. Atmos.* **126** e2019JD032361
- [83] Terhaar J, Frölicher T L and Joos F 2023 *Projected ocean carbon cycle and ocean acidification for given temperature targets from Bern3D-LPX simulations with the AERA (SEANOE)* (<https://doi.org/10.17882/92735>)
- [84] Torres O, Kwiatkowski L, Sutton A J, Dorey N and Orr J C 2021 Characterizing mean and extreme diurnal variability of ocean CO<sub>2</sub> system variables across marine environments *Geophys. Res. Lett.* **48** e2020GL090228
- [85] Kwiatkowski L, Torres O, Aumont O and Orr J C 2022 Modified future diurnal variability of the global surface ocean CO<sub>2</sub> system *Glob. Change Biol.* **1**–16
- [86] Hauri C, Friedrich T and Timmermann A 2016 Abrupt onset and prolongation of aragonite undersaturation events in the Southern Ocean *Nat. Clim. Change* **6** 172–6
- [87] Berge J *et al* 2015 In the dark: a review of ecosystem processes during the Arctic polar night *Prog. Oceanogr.* **139** 258–71
- [88] Terhaar J, Tanhua T, Stöven T, Orr J C and Bopp L 2020 Evaluation of data-based estimates of anthropogenic carbon in the Arctic Ocean *J. Geophys. Res. Ocean* **125** e2020JC016124
- [89] Resplandy L, Bopp L, Orr J C and Dunne J P 2013 Role of mode and intermediate waters in future ocean acidification: analysis of CMIP5 models *Geophys. Res. Lett.* **40** 3091–5
- [90] Goris N, Tjiputra J F, Olsen A, Schwinger J, Lauvset S K and Jeansson E 2018 Constraining projection-based estimates of the future north Atlantic carbon uptake *J. Clim.* **31** 3959–78
- [91] Bourgeois T, Goris N, Schwinger J and Tjiputra J F 2022 Stratification constrains future heat and carbon uptake in the Southern Ocean between 30°S and 55°S *Nat. Commun.* **13** 340
- [92] Lauvset S K *et al* 2016 A new global interior ocean mapped climatology: the 11 GLODAP version 2 *Earth Syst. Sci. Data* **8** 325–40
- [93] Meinshausen M, Lewis J, McGlade C, Gütschow J, Nicholls Z, Burdon R, Cozzi L and Hackmann B 2022 Realization of Paris Agreement pledges may limit warming just below 2 °C *Nature* **604** 304–9
- [94] Hauri C, Pagès R, McDonnell A M P, Stuecker M F, Danielson S L, Hedstrom K, Irving B, Schultz C and Doney S C 2021 Modulation of ocean acidification by decadal climate variability in the Gulf of Alaska *Commun. Earth Environ.* **2** 191
- [95] Gruber N, Hauri C, Lachkar Z, Loher D, Frölicher T L and Plattner G-K 2012 Rapid progression of Ocean acidification in the California Current System *Science* **337** 220–3
- [96] Franco A C, Gruber N, Frölicher T L and Kropuenske Artman L 2018 Contrasting impact of future CO<sub>2</sub> emission scenarios on the extent of CaCO<sub>3</sub> mineral undersaturation in the Humboldt current system *J. Geophys. Res. Ocean* **123** 2018–36
- [97] Griffies S M *et al* 2015 Impacts on Ocean heat from transient mesoscale eddies in a hierarchy of climate models *J. Clim.* **28** 952–77
- [98] Dufour C O *et al* 2015 Role of mesoscale eddies in cross-frontal transport of Heat and Biogeochemical Tracers in the Southern Ocean *J. Phys. Oceanogr.* **45** 3057–81
- [99] Lachkar Z, Orr J C and Dutay J-C 2009 Seasonal and mesoscale variability of oceanic transport of anthropogenic CO<sub>2</sub> *Biogeosciences* **6** 2509–23